Published in final edited form as:
J Cell Biochem. 2014 January ; 115(1): 179–188. doi:10.1002/jcb.24648.

Roles of Parathyroid Hormone (PTH) Receptor and Reactive Oxygen Species in Hyperlipidemia-Induced PTH(1-34) Resistance in Preosteoblasts.

Xin Li[1,#], **Jamie Garcia**[1,#], **Jinxiu Lu**[2], **Sidney Iriana**[1], **Ivo Kalajzic**[3], **David Rowe**[3], **Linda Demer**[1,2,4], and **Yin Tintut**[1,*]

[1]Department of Medicine, University of California, Los Angeles, California

[2]Department of Physiology, University of California, Los Angeles, California

[4]Department of Bioengineering, University of California, Los Angeles, California

[3]University of Connecticut Health Center, Farmington, Connecticut

Abstract

Bioactive lipids initiate inflammatory reactions leading to pathogenesis of atherosclerosis. Evidence shows that they also contribute to bone loss by inhibiting parathyroid hormone receptor (PTH1R) expression and differentiation of osteoblasts. We previously demonstrated that bone anabolic effects of PTH(1-34) are blunted in hyperlipidemic mice and that these PTH effects are restored by antioxidants. However, it is not clear which osteoblastic cell developmental stage is targeted by bioactive lipids. To investigate the effects of hyperlipidemia at the cellular level, hyperlipidemic *Ldlr*$^{-/-}$ mice were bred with Col3.6GFPtpz mice, in which preosteoblasts/osteoblasts carry a topaz fluorescent label, and with Col2.3GFPcyan mice, in which more mature osteoblasts/osteocytes carry a cyan fluorescent label. Histological analyses of trabecular bone surfaces in femoral as well as calvarial bones showed that intermittent PTH(1-34) increased fluorescence intensity in WT-Tpz mice, but not in Tpz-*Ldlr*$^{-/-}$ mice. In contrast, PTH(1-34) did not alter fluorescence intensity in femoral cortical envelopes of either WT-Cyan or *Ldlr*$^{-/-}$-Cyan mice. To test the mechanism of PTH1R downregulation, preosteoblastic MC3T3-E1 cells were treated with bioactive lipids and the antioxidant Trolox. Results showed that inhibitory effects of PTH1R levels by bioactive lipids were rescued by pretreatment with Trolox. The inhibitory effects on expression of PTH1R as well as on PTH-induced osteoblastic genes were mimicked by xanthine/xanthine oxidase, a known generator of reactive oxygen species. These findings suggest an important role of preosteoblasts as the target development stage and downregulation of PTH receptor expression mediated by intracellular oxidant stress as a mechanism in hyperlipidemia-induced PTH resistance.

Keywords

Hyperlipidemia; bioactive lipids; preosteoblasts; PTH receptor; reactive oxygen species

Epidemiological studies suggest that osteoporosis and vertebral fractures associate with cardiovascular disease [Barengolts et al., 1998; Hjortnaes et al., 2010; Kiel et al., 2001;

To whom correspondence should be addressed: Yin Tintut, The David Geffen School of Medicine, University of California, Los Angeles, Center for the Health Sciences A2-237, 10833 Le Conte Ave, Los Angeles, CA. 90095-1679, Phone: (310) 206-9964, fax: (310) 825-4963, ytintut@mednet.ucla.edu.
[#]Equal contributors

Pennisi et al., 2004; Schulz et al., 2004; Tamaki et al., 2009] and that the association is independent of age [Boukhris and Becker, 1972; Frye et al., 1992]. Evidence shows that lipid oxidation products trigger a cascade of inflammatory reactions responsible for the pathogenesis of cardiovascular diseases, particularly atherosclerosis [Morgantini et al., 2010; Navab et al., 1996; Towler, 2008].

Lipid oxidation products may also contribute to similar pathological events resulting in bone loss. Histochemical evidence demonstrates accumulation of lipids in the subendothelial space of Haversian cannels of human osteoporotic bones [Tintut et al., 2004] and in osteocytic canaliculae [Kawai et al., 1980; Watanabe et al., 1989]. Levels of lipid oxidation products are also increased in plasma [Pirih et al.] and in the bone marrow of hyperlipidemic mice fed an atherogenic high-fat diet [Tintut et al., 2004] that is known to induce bone loss [Hirasawa et al., 2007; Hjortnaes et al., 2010; Pirih et al.]. In vivo animal studies demonstrate that bioactive lipids mediate adverse effects of the atherogenic diet on bone [Sage et al., 2011] and that the effects may be through inhibition of osteoblastic differentiation of preosteoblasts and bone marrow stromal cells [Parhami et al., 1999; Parhami et al., 1997] as well as through lowering expression of parathyroid hormone receptor (PTH1R) [Pirih et al.]. In mice, hyperlipidemia also interfere with the bone anabolic effects of PTH(1-34) [Huang et al., 2008a], a treatment widely used for treating patients with osteoporosis [Iida-Klein et al., 2002; Lindsay et al., 1997]. In support of the animal studies, a recent retrospective, longitudinal study found that levels of total cholesterol correlate negatively, and levels of HDL cholesterol correlate positively, with lumbar bone mineral density in patients, who were treated with teriparatide (PTH 1-34) [Jeon et al., 2013].

Oxidant stress has been shown to play a central role in pathogenesis of atherosclerosis [Morrow, 2005; Yokoyama, 2004]. In osteoblasts, increased lipid oxidation also triggers cellular oxidant stress [Almeida et al., 2009; Mody et al., 2001]. Modulation of oxidative stress also affects bone mass homeostasis [Ambrogini et al.; Rached et al.]. We have previously found that lowering oxidant stress in hyperlipidemic low-density receptor null ($Ldlr^{-/-}$) mice, by administration of an ApoA-I mimetic peptide [Sage et al., 2011] or by overexpression of paraoxonase 1 gene, restores the bone anabolic effects of PTH(1-34) [Lu et al., 2013]. Administration of PTH(1-34) had greater bone anabolic effects in aged mice compared with younger mice due to the age-associated increase in oxidant stress [Jilka et al., 2010].

PTH anabolic effects have been attributed, in part, to proliferation of osteoblasts [Cipriani et al., 2012]. Using cells isolated from the transgenic mice, where green fluorescent protein (GFP) expression is driven by either a 3.6-kilobase (kb; pOBCol3.6GFPtpz) or 2.3-kb (pOBCol2.3GFPcyan) promoter fragment of rat type I collagen, Kalajzic and colleagues showed that the 3.6-kb type I collagen promoter marks osteoblast lineage cells at the stage of preosteoblasts and immature osteoblasts (here labeled with a topaz fluorescent reporter), whereas the 2.3-kb promoter marks more mature osteoblasts and osteocytes (here labeled with a cyan fluorescent reporter) [Kalajzic et al., 2002]. In bone tissue from the transgenic mice, GFP expression in pOBCol3.6GFPtpz was observed in osteoblastic cells lining endosteal and trabecular surfaces, whereas GFP expression in pOBCol2.3GFPcyan was observed in osteoblasts and osteocytes [Kalajzic et al., 2002]. In this report, we sought to identify which osteoblastic developmental level is the target of hyperlipidemia-induced PTH resistance using hyperlipidemic or WT mice expressing GFP from pOBCol3.6GFPtpz or pOBCol2.3GFPcyan. We also examined whether the inhibitory effects of inflammatory bioactive lipids on PTH1R is mediated by ROS in preosteoblasts.

METHODS

Materials

8-Isoprostaglandin E2 (isoPGE2) was purchased from Cayman Chemical (Ann Arbor, MI). Xanthine, xanthine oxidase, Trolox (6-hydroxy-2, 5, 7, 8-tetramethylchroman-2-carboxylic acid) and human PTH(1-34) were purchased from Sigma. Oxidized 1-palmitoyl-2-arachidonyl-sn-glycero-3-phosphocholine (ox-PAPC) was prepared by auto-oxidation of PAPC (Avanti-Polar Lipids). The oxidation state was verified by liquid chromatography/mass spectroscopy.

Mice

Mice (C57BL/6 background) overexpressing GFP from Colla1 promoter fragments (pOBCol3.6GFPtpz and pOBCol2.3GFPCyan) were generated, as described previously [Kalajzic et al., 2002]. The mice were bred with low-density lipoprotein receptor (*Ldlr*) null mice (Jackson Laboratory) to produce hyperlipidemic mice that express GFP in preosteoblasts, immature osteoblasts as well as osteoblasts and osteocytes. No differences in health or development between hyperlipidemic and wild type GFP mice were observed. The pups were verified by genotyping tails for the presence of GFP and absence of Ldlr, using protocols established by the Rowe/Kalajzic laboratories and the Jackson Laboratory, respectively. Mice with homozygosity for the Ldlr null mutation and positive for GFP were selected for further experiments. All the experimental protocols were reviewed and approved by the Institutional Animal Care and Use Committee of the University of California at Los Angeles.

Intermittent PTH treatment

Female mice (2–3 months old) and littermates (n = 6–8/group) were injected with either control vehicle or human PTH (1-34; 40 μg/kg, *s.c.* 5 days/wk) for 5 wks, as previously described [Huang et al., 2008a; Sage et al., 2011].

Histological evaluation

At euthanasia, calvarias and left femurs were harvested, cleaned of surrounding tissue for femoral bones and immediately fixed in 10% formalin for 48 hours in 4°C. The bones were subsequently decalcified for 4–7 days in 14% EDTA (pH 7.1), incubated in 30% sucrose for 24 hours, and embedded in OCT. Endogenous fluorescence from 3 serial sections of calvarial bones was imaged using TPZ filter (Olympus). Approximately 10 μ-thick longitudinal sections of femoral bones were sectioned onto 2 cm cyrofilms (Molecular Core, University of Connecticut Health Center, Farmington, CT). To improve the signal-to-noise ratio for femoral bones, instead of directly imaging GFPtpz and GFPcyan fluorescence, we performed immunostaining with anti-GFP antibody conjugated with Alexa Fluor® 594 (Life Technologies). Three serial sections of femoral bones were analyzed. Images of the distal femurs and calvarial bones were quantified as percentage of tissue area in 3 sections per mouse bone, using image analysis software (Metamorph Advanced *v7.7*), as we previously described [Lu et al., 2013].

Cell culture

Preosteoblasts MC3T3-E1 mouse cell line (Riken Cell Bank) were grown in alpha-MEM (Cellgrow) containing 10% FBS, supplemented with sodium pyruvate (1 mmol/L), penicillin (100 U/mL) and streptomycin (100 U/mL). Cells were treated at subconfluence in alpha-MEM media supplemented with 2.5% FBS, 5 mM beta-glycerolphosphate and 50 μg/ml ascorbic acid at the indicated time points. Media supplemented with fresh agents were replenished every 3–4 days.

Alkaline phosphatase activity assay

Alkaline phosphatase activity was assayed in whole cell lysates, as previously described [Huang et al., 2008b].

Realtime RT-qPCR

Total RNA was isolated and realtime RT-qPCR was performed using the One-Step RT-qPCR SuperMix Kit (SYBR green, BioChain, Inc.) and Mx3005P Real-Time PCR System (Stratagene).

Immunofluorescence

The cells were plated in 8-well chamber slides and treated with the indicated reagents for 6 days. The cells were washed, fixed, and incubated overnight with anti-PTH1R antibody (Covance, Emeryville, CA). The PTH1R staining was visualized using secondary antibody conjugated with Alexa Fluor 488 (Invitrogen). The PTH1R-stained cells were imaged and quantified by normalizing for cell number (≥ 4 fields) using image analysis software (Metamorph Advanced *v7.7*), as we previously described [Lu et al., 2013].

Dihydroethidium (DHE) staining

The cells were plated in 8-well chamber slides and treated with vehicle or isoPGE2 at subconfluence in the alpha-MEM containing DHE (30 μM, Sigma) for 10 min in a 37°C incubator. After the incubation the media was removed, washed twice with PBS, and mounted. DHE-stained cells were imaged and quantified by normalizing for cell number (≥ 4 fields) using image analysis software (Metamorph Advanced *v7.7*), as we previously described [Lu et al., 2013].

Statistical analysis

Values were expressed as mean ± SEM. Statistical significance was determined by Student's *t*-test, with a value of $p < 0.05$ considered significant. For comparisons between more than two groups, *p* values were calculated using ANOVA and Fisher's projected least significant difference (PLSD) significance test (StatView 4.5).

RESULTS

Effects of PTH(1-34) on GFP-labeled osteoblasts and osteocytes

We previously found that bone anabolic effects of PTH(1-34) were blunted in hyperlipidemic (*Ldlr*$^{-/-}$) mice [Huang et al., 2008a]. To identify the osteoblast developmental stage affected by hyperlipidemia-induced PTH resistance, two lines of GFP mice (GFPTpz that label preosteoblasts/osteoblasts and GFPCyan that label osteocytes) were bred with hyperlipidemic (*Ldlr*$^{-/-}$) mice to produce Tpz-*Ldlr*$^{-/-}$ and Cyan-*Ldlr*$^{-/-}$ mice. Intermittent PTH(1-34) treatment (5 days/week, *s.c.*) was administered to Tpz-*Ldlr*$^{-/-}$ and Cyan-*Ldlr*$^{-/-}$ as well as their littermates (Tpz-WT and Cyan-WT). After 5 weeks of PTH treatment, long bones and calvarias were harvested, and the effects of PTH(1-34) were analyzed.

To visualize the cell type affected by PTH(1-34), histological evaluation of GFP-labeled osteoblast lineage cells on the trabecular surfaces of femoral bones was performed. To improve the signal-to-noise ratio for femoral bones, we performed immunofluorescence using anti-GFP antibody conjugated with Alexa Fluor® 594. As shown in Figure 1A–B, PTH(1-34) treatment increased the fluorescence intensity in WT mice. In contrast, the effect of PTH treatment was blunted in *Ldlr*$^{-/-}$ mice (Fig. 1A–B). Epifluorescence analysis of

GFPtpz in the calvarial bones of TPZ mice also showed that PTH induction of fluorescence intensity was blunted in *Ldlr*$^{-/-}$ mice (Fig. 2A–B).

To assess the effects of PTH treatment on osteocytes, fluorescently labeled osteocytes of the femoral bones were assessed in Cyan mice. As shown in Figure 3A–B, PTH treatment did not increase the immunofluorescence intensity in WT or *Ldlr*$^{-/-}$ mice.

ROS mediates effects of bioactive inflammatory lipids on PTH1R levels

To determine the mechanism of the effects of inflammatory lipids on PTH receptor levels, MC3T3-E1 cells, the established preosteoblasts, were treated with a bioactive lipid, 8-isoprostaglandin E2 (isoPGE2). As shown in Figure 4A–B, isoPGE2 reduced expression of PTH1R, as assessed by immunocytochemistry.

We next examined whether inhibitory effects of lipids on PTH1R expression and responsiveness to PTH(1-34) treatment were mediated by intracellular ROS. Cells were treated with 8-isoprostaglandin E2 (isoPGE2) and ROS production was assessed. Results show that levels of the intracellular ROS were increased in cells treated with isoPGE2 compared with controls (Fig. 5A–B).

The direct effects of ROS on PTH1R expression was tested by treating the cells for 6 days with xanthine/xanthine oxidase (X/XO), which generates superoxide anion. Realtime RT-qPCR analysis shows that the inhibitory effect on PTH1R expression was also mimicked by X/XO treatment (Figure 6A–C).

To test whether ROS inhibition of PTH1R expression had effects on the response of osteoblasts to PTH treatment, the cells were pretreated with XXO for 6 days, and stimulated with PTH(1-34) at day 6 for 1.5 hr. Results from realtime RT-qPCR analysis showed reduced expression of PTH-induced Nurr1, an immediate early gene, after the XXO pretreatment (Fig. 7A). PTH induction of osteoblastic differentiation markers, bone sialoprotein and osteocalcin, was also blunted by the X/XO pre-treatment (Fig. 7B–C). In contrast, co-treatment of PTH with X/XO did not inhibit PTH induction of Nurr1 or osteocalcin (Fig. 7D–E).

We previously found that treatment with antioxidant D4-F [Sage et al., 2011] or in transgenic hyperlipidemic mice expressing antioxidant human paraoxonase 1 [Lu et al., 2013], PTH(1-34) response to BMD was also recovered [Lu et al., 2013; Sage et al., 2011]. Therefore, we used a known anti-oxidant, Trolox, to block the inhibitory effects of isoPGE2. As shown in Figure 5A, treatment with Trolox blocked the inhibitory effects of isoPGE2 on ALP activity (Fig. 8A). In addition, pretreatment for 1 hr with Trolox also ameliorated the inhibitory effects of PTH1R expression by bioactive lipids (Fig. 8B–D).

DISCUSSION

We previously found that bioactive inflammatory lipids inhibit PTH receptor (PTH1R) expression [Huang et al., 2007] and that PTH1R expression is also lower in hyperlipidemic than WT mice [Pirih et al., 2012; Sage et al., 2011]. In subsequent experiments, we showed that bone anabolic effects of PTH(1-34) are blunted in hyperlipidemic mice [Huang et al., 2008a]. As evidence that these findings translate to human disease, the recent clinical study by Jeon et al. [Jeon et al., 2013] revealed that high total cholesterol levels significantly associate with blunted effects, and HDL levels with enhanced effects, of teriparatide in patients. The present results now suggest a novel mechanism in which preosteoblasts, but not osteocytes, are selectively targeted and in which ROS mediate the adverse effects of the lipids by inhibiting PTH receptor expression.

In our previous studies, we found that inflammatory lipids induce oxidant stress by inducing intracellular ROS production in osteoblastic cells and that the differentiation of osteoblastic cells is inhibited by ROS generating agents [Mody et al., 2001]. We now show that intracellular ROS also mediate the downregulation of PTH1R by inflammatory lipids. The reduced expression of PTH1R was confirmed by the blunted PTH responsiveness to expression of a downstream PTH target genes only when cells were pretreated with xanthine/xanthine oxidase. These findings suggest that blunting of PTH anabolism in hyperlipidemic mice may result, in part, from the decrease in receptor levels. The results are also in agreement with our recent report that shows that, overexpression of the antioxidant enzyme paraoxonase-1 in *Ldlr*$^{-/-}$ mice rescues PTH1R expression relative to their littermates, *Ldlr*$^{-/-}$ mice [Lu et al., 2013].

Bone anabolic effects of PTH(1-34) have been attributed in part to effects on proliferation of osteoblast progenitor cells and conversion of bone lining cells to osteoblasts [Luiz de Freitas et al., 2009; Nishida et al., 1994]. Recently studies by Kim and colleagues (2012) showed that intermittent PTH treatment promotes the maturation of osteoblasts in mice [Kim et al., 2012]. Using osteoblasts labeled with GFP driven by the 3.6 kb Col1a1 promoter, Wang and colleagues [Wang et al., 2007] showed that early transient PTH treatment enhanced the commitment of osteoprogenitor cells to a differentiated osteoblast phenotype. Consistent with this study, we found in vivo that intermittent PTH(1-34) treatment enhanced osteoblastic differentiation as evidenced by increased fluorescence intensity in WT mice expressing Tpz label driven from the 3.6 kb Col1a1 promoter, suggesting that PTH affects early stages of osteoblast development. In contrast, when the mice were hyperlipidemic due to LDL receptor deficiency (Col3.6 Tpz; *Ldlr*$^{-/-}$) mice, the PTH effect was blunted, suggesting that inflammatory lipids, in part, target osteoblastic cells at the stages of preosteoblasts and immature osteoblasts.

Responses of osteocytic cells to PTH differ from those of the more immature osteoblasts. These cells fail to increase their collagen expression driven from the 2.3kb promoter fragment in response to PTH in both WT and *Ldlr*$^{-/-}$ mice. However, it remains possible that other functions of the osteocytes, such as sclerostin expression, may still be responding to PTH in the WT mice. Indeed, we previously found that sclerostin expression was responsive to PTH in paraoxonase overexpressing *Ldlr*$^{-/-}$ mice [Lu et al., 2013]. This is consistent with prior studies [O'Brien et al., 2008; Rhee et al., 2011] showing that osteocytes control bone remodeling via PTH signaling and that PTH affects sclerostin expression [Weinstein et al., 2010].

In summary, the present findings suggest an important role of preosteoblasts and immature osteoblasts as the target cells and downregulation of PTH receptor expression mediated by intracellular oxidant stress as the mechanisms in hyperlipidemia-induced PTH resistance.

Acknowledgments

Contract grant number: The National Institutes of Health (DK081346, DK081346-S1, HL114709, and the National Center for Advancing Translational Sciences UCLA CTSI Grant UL1TR000124, T32 GM055052).

This work was supported by funding from the National Institutes of Health (DK081346, DK081346-S1, HL114709, and the National Center for Advancing Translational Sciences UCLA CTSI Grant UL1TR000124, T32 GM055052).

References

Almeida M, Ambrogini E, Han L, Manolagas SC, Jilka RL. Increased lipid oxidation causes oxidative stress, increased peroxisome proliferator-activated receptor-gamma expression, and diminished pro-osteogenic Wnt signaling in the skeleton. J Biol Chem. 2009; 284:27438–48. [PubMed: 19657144]

Ambrogini E, Almeida M, Martin-Millan M, Paik JH, Depinho RA, Han L, Goellner J, Weinstein RS, Jilka RL, O'Brien CA, Manolagas SC. FoxO-mediated defense against oxidative stress in osteoblasts is indispensable for skeletal homeostasis in mice. Cell Metab. 2010; 11:136–46. [PubMed: 20142101]

Barengolts EI, Berman M, Kukreja SC, Kouznetsova T, Lin C, Chomka EV. Osteoporosis and coronary atherosclerosis in asymptomatic postmenopausal women. Calcif Tissue Int. 1998; 62:209–13. [PubMed: 9501953]

Boukhris R, Becker KL. Calcification of the aorta and osteoporosis. A roentgenographic study. JAMA. 1972; 219:1307–11. [PubMed: 5066773]

Cipriani C, Irani D, Bilezikian JP. Safety of osteoanabolic therapy: a decade of experience. J Bone Miner Res. 2012; 27:2419–28. [PubMed: 23165426]

Frye MA, Melton LJ 3rd, Bryant SC, Fitzpatrick LA, Wahner HW, Schwartz RS, Riggs BL. Osteoporosis and calcification of the aorta. Bone Miner. 1992; 19:185–94. [PubMed: 1422314]

Hirasawa H, Tanaka S, Sakai A, Tsutsui M, Shimokawa H, Miyata H, Moriwaki S, Niida S, Ito M, Nakamura T. ApoE gene deficiency enhances the reduction of bone formation induced by a high-fat diet through the stimulation of p53-mediated apoptosis in osteoblastic cells. J Bone Miner Res. 2007; 22:1020–30. [PubMed: 17388726]

Hjortnaes J, Butcher J, Figueiredo JL, Riccio M, Kohler RH, Kozloff KM, Weissleder R, Aikawa E. Arterial and aortic valve calcification inversely correlates with osteoporotic bone remodelling: a role for inflammation. Eur Heart J. 2010; 31:1975–84. [PubMed: 20601388]

Huang MS, Lu J, Ivanov Y, Sage AP, Tseng W, Demer LL, Tintut Y. Hyperlipidemia impairs osteoanabolic effects of PTH. J Bone Miner Res. 2008a; 23:1672–9. [PubMed: 18505371]

Huang MS, Morony S, Lu J, Zhang Z, Bezouglaia O, Tseng W, Tetradis S, Demer LL, Tintut Y. Atherogenic phospholipids attenuate osteogenic signaling by BMP-2 and parathyroid hormone in osteoblasts. J Biol Chem. 2007; 282:21237–43. [PubMed: 17522049]

Huang MS, Sage AP, Lu J, Demer LL, Tintut Y. Phosphate and pyrophosphate mediate PKA-induced vascular cell calcification. Biochem Biophys Res Commun. 2008b; 374:553–8. [PubMed: 18655772]

Iida-Klein A, Zhou H, Lu SS, Levine LR, Ducayen-Knowles M, Dempster DW, Nieves J, Lindsay R. Anabolic action of parathyroid hormone is skeletal site specific at the tissue and cellular levels in mice. J Bone Miner Res. 2002; 17:808–16. [PubMed: 12009011]

Jeon YK, Kim KM, Kim KJ, Kim IJ, Lim SK, Rhee Y. The Anabolic Effect of Teriparatide is Undermined by Low Levels of High-Density Lipoprotein Cholesterol. Calcif Tissue Int. 2013

Jilka RL, Almeida M, Ambrogini E, Han L, Roberson PK, Weinstein RS, Manolagas SC. Decreased oxidative stress and greater bone anabolism in the aged, when compared to the young, murine skeleton with parathyroid hormone administration. Aging Cell. 2010; 9:851–67. [PubMed: 20698835]

Kalajzic I, Kalajzic Z, Kaliterna M, Gronowicz G, Clark SH, Lichtler AC, Rowe D. Use of type I collagen green fluorescent protein transgenes to identify subpopulations of cells at different stages of the osteoblast lineage. J Bone Miner Res. 2002; 17:15–25. [PubMed: 11771662]

Kawai K, Maruno H, Watanabe Y, Hirohata K. Fat necrosis of osteocytes as a causative factor in idiopathic osteonecrosis in heritable hyperlipemic rabbits. Clin Orthop Relat Res. 1980:273–82. [PubMed: 7449227]

Kiel DP, Kauppila LI, Cupples LA, Hannan MT, O'Donnell CJ, Wilson PW. Bone loss and the progression of abdominal aortic calcification over a 25 year period: the Framingham Heart Study. Calcif Tissue Int. 2001; 68:271–6. [PubMed: 11683533]

Kim SW, Pajevic PD, Selig M, Barry KJ, Yang JY, Shin CS, Baek WY, Kim JE, Kronenberg HM. Intermittent parathyroid hormone administration converts quiescent lining cells to active osteoblasts. J Bone Miner Res. 2012; 27:2075–84. [PubMed: 22623172]

Lindsay R, Nieves J, Formica C, Henneman E, Woelfert L, Shen V, Dempster D, Cosman F. Randomised controlled study of effect of parathyroid hormone on vertebral-bone mass and fracture incidence among postmenopausal women on oestrogen with osteoporosis. Lancet. 1997; 350:550–5. [PubMed: 9284777]

Lu J, Cheng H, Atti E, Shih DM, Demer LL, Tintut Y. Role of paraoxonase-1 in bone anabolic effects of parathyroid hormone in hyperlipidemic mice. Biochem Biophys Res Commun. 2013 In Press.

Luiz de Freitas PH, Li M, Ninomiya T, Nakamura M, Ubaidus S, Oda K, Udagawa N, Maeda T, Takagi R, Amizuka N. Intermittent PTH administration stimulates pre-osteoblastic proliferation without leading to enhanced bone formation in osteoclast-less c-fos(−/−) mice. J Bone Miner Res. 2009; 24:1586–97. [PubMed: 19419301]

Mody N, Parhami F, Sarafian TA, Demer LL. Oxidative stress modulates osteoblastic differentiation of vascular and bone cells. Free Radic Biol Med. 2001; 31:509–19. [PubMed: 11498284]

Morgantini C, Imaizumi S, Grijalva V, Navab M, Fogelman AM, Reddy ST. Apolipoprotein A-I mimetic peptides prevent atherosclerosis development and reduce plaque inflammation in a murine model of diabetes. Diabetes. 2010; 59:3223–8. [PubMed: 20826564]

Morrow JD. Quantification of isoprostanes as indices of oxidant stress and the risk of atherosclerosis in humans. Arterioscler Thromb Vasc Biol. 2005; 25:279–86. [PubMed: 15591226]

Navab M, Berliner JA, Watson AD, Hama SY, Territo MC, Lusis AJ, Shih DM, Van Lenten BJ, Frank JS, Demer LL, Edwards PA, Fogelman AM. The Yin and Yang of oxidation in the development of the fatty streak. A review based on the 1994 George Lyman Duff Memorial Lecture. Arterioscler Thromb Vasc Biol. 1996; 16:831–42. [PubMed: 8673557]

Nishida S, Yamaguchi A, Tanizawa T, Endo N, Mashiba T, Uchiyama Y, Suda T, Yoshiki S, Takahashi HE. Increased bone formation by intermittent parathyroid hormone administration is due to the stimulation of proliferation and differentiation of osteoprogenitor cells in bone marrow. Bone. 1994; 15:717–23. [PubMed: 7873302]

O'Brien CA, Plotkin LI, Galli C, Goellner JJ, Gortazar AR, Allen MR, Robling AG, Bouxsein M, Schipani E, Turner CH, Jilka RL, Weinstein RS, Manolagas SC, Bellido T. Control of bone mass and remodeling by PTH receptor signaling in osteocytes. PLoS One. 2008; 3:e2942. [PubMed: 18698360]

Parhami F, Jackson SM, Tintut Y, Le V, Balucan JP, Territo M, Demer LL. Atherogenic diet and minimally oxidized low density lipoprotein inhibit osteogenic and promote adipogenic differentiation of marrow stromal cells. J Bone Miner Res. 1999; 14:2067–78. [PubMed: 10620066]

Parhami F, Morrow AD, Balucan J, Leitinger N, Watson AD, Tintut Y, Berliner JA, Demer LL. Lipid oxidation products have opposite effects on calcifying vascular cell and bone cell differentiation. A possible explanation for the paradox of arterial calcification in osteoporotic patients. Arterioscler Thromb Vasc Biol. 1997; 17:680–7. [PubMed: 9108780]

Pennisi P, Signorelli SS, Riccobene S, Celotta G, Di Pino L, La Malfa T, Fiore CE. Low bone density and abnormal bone turnover in patients with atherosclerosis of peripheral vessels. Osteoporos Int. 2004; 15:389–95. [PubMed: 14661073]

Pirih F, Lu J, Ye F, Bezouglaia O, Atti E, Ascenzi M, Tetradis S, Demer L, Aghaloo T, Tintut Y. Adverse effects of hyperlipidemia on bone regeneration and strength. J Bone Miner Res. 2012; 27(2):309–18. [PubMed: 21987408]

Rached MT, Kode A, Xu L, Yoshikawa Y, Paik JH, Depinho RA, Kousteni S. FoxO1 is a positive regulator of bone formation by favoring protein synthesis and resistance to oxidative stress in osteoblasts. Cell Metab. 11:147–60. [PubMed: 20142102]

Rhee Y, Allen MR, Condon K, Lezcano V, Ronda AC, Galli C, Olivos N, Passeri G, O'Brien CA, Bivi N, Plotkin LI, Bellido T. PTH receptor signaling in osteocytes governs periosteal bone formation and intracortical remodeling. J Bone Miner Res. 2011; 26:1035–46. [PubMed: 21140374]

Sage AP, Lu J, Atti E, Tetradis S, Ascenzi MG, Adams DJ, Demer LL, Tintut Y. Hyperlipidemia induces resistance to PTH bone anabolism in mice via oxidized lipids. J Bone Miner Res. 2011; 26:1197–206. [PubMed: 21611962]

Schulz E, Arfai K, Liu X, Sayre J, Gilsanz V. Aortic calcification and the risk of osteoporosis and fractures. J Clin Endocrinol Metab. 2004; 89:4246–53. [PubMed: 15356016]

Tamaki J, Iki M, Hirano Y, Sato Y, Kajita E, Kagamimori S, Kagawa Y, Yoneshima H. Low bone mass is associated with carotid atherosclerosis in postmenopausal women: the Japanese Population-based Osteoporosis (JPOS) Cohort Study. Osteoporos Int. 2009; 20:53–60. [PubMed: 18496639]

Tintut Y, Morony S, Demer LL. Hyperlipidemia promotes osteoclastic potential of bone marrow cells ex vivo. Arterioscler Thromb Vasc Biol. 2004; 24:e6–10. [PubMed: 14670933]

Towler DA. Oxidation, inflammation, and aortic valve calcification peroxide paves an osteogenic path. J Am Coll Cardiol. 2008; 52:851–4. [PubMed: 18755349]

Wang YH, Liu Y, Rowe DW. Effects of transient PTH on early proliferation, apoptosis, and subsequent differentiation of osteoblast in primary osteoblast cultures. Am J Physiol Endocrinol Metab. 2007; 292:E594–603. [PubMed: 17032929]

Watanabe Y, Kawai K, Hirohata K. Histopathology of femoral head osteonecrosis in rheumatoid arthritis: the relationship between steroid therapy and lipid degeneration in the osteocyte. Rheumatol Int. 1989; 9:25–31. [PubMed: 2772484]

Weinstein RS, Jilka RL, Almeida M, Roberson PK, Manolagas SC. Intermittent parathyroid hormone administration counteracts the adverse effects of glucocorticoids on osteoblast and osteocyte viability, bone formation, and strength in mice. Endocrinology. 2010; 151:2641–9. [PubMed: 20410195]

Yokoyama M. Oxidant stress and atherosclerosis. Curr Opin Pharmacol. 2004; 4:110–5. [PubMed: 15063353]

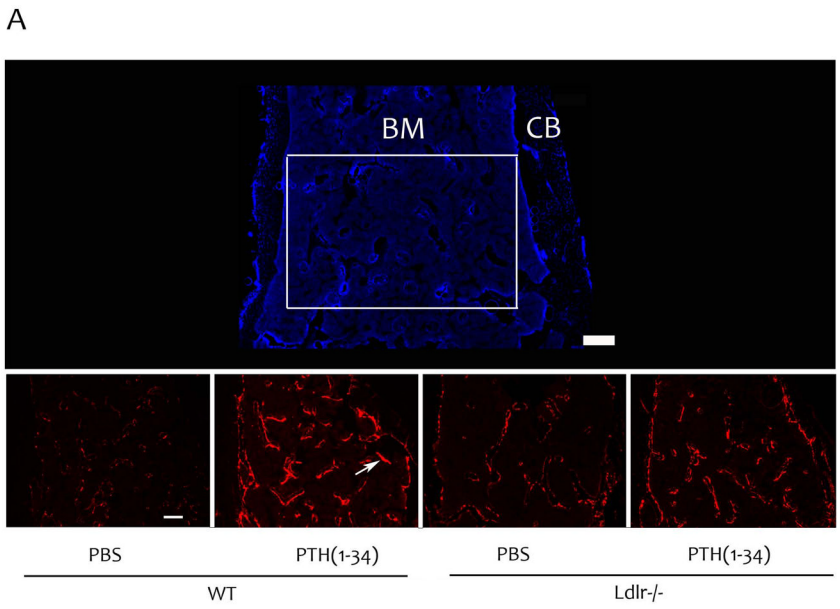

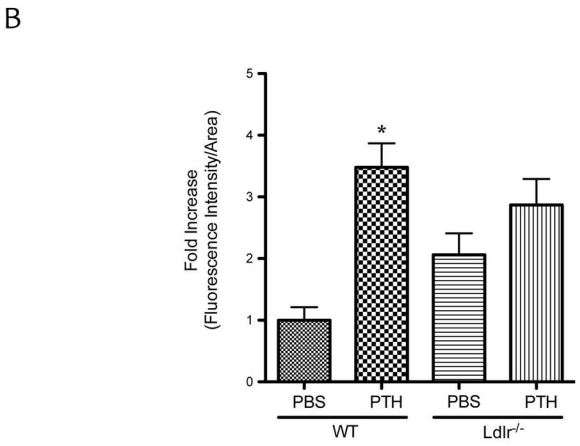

Figure 1. Effects of PTH(1-34) on GFP-labeled osteoblasts in femoral bone

(A) Top panel –The DAPI image of distal femoral bone from Tpz mice [bone marrow (BM), cortical bone (CB)]. Bottom panels – immuno-fluorescence images of the area marked by the white rectangular box in panel A using anti-GFP antibody (rather than direct fluorescence from GFPtpz for enhanced signal-to-noise ratio). Arrow indicates fluorescence labeled osteoblasts lining the trabecular surface. (B) Quantitation by Metamorph image analysis of the area shown in the bottom panels in (A). Magnification bar − 200 μm. $^{*}p <$ 0.05 vs. respective PBS-treated controls.

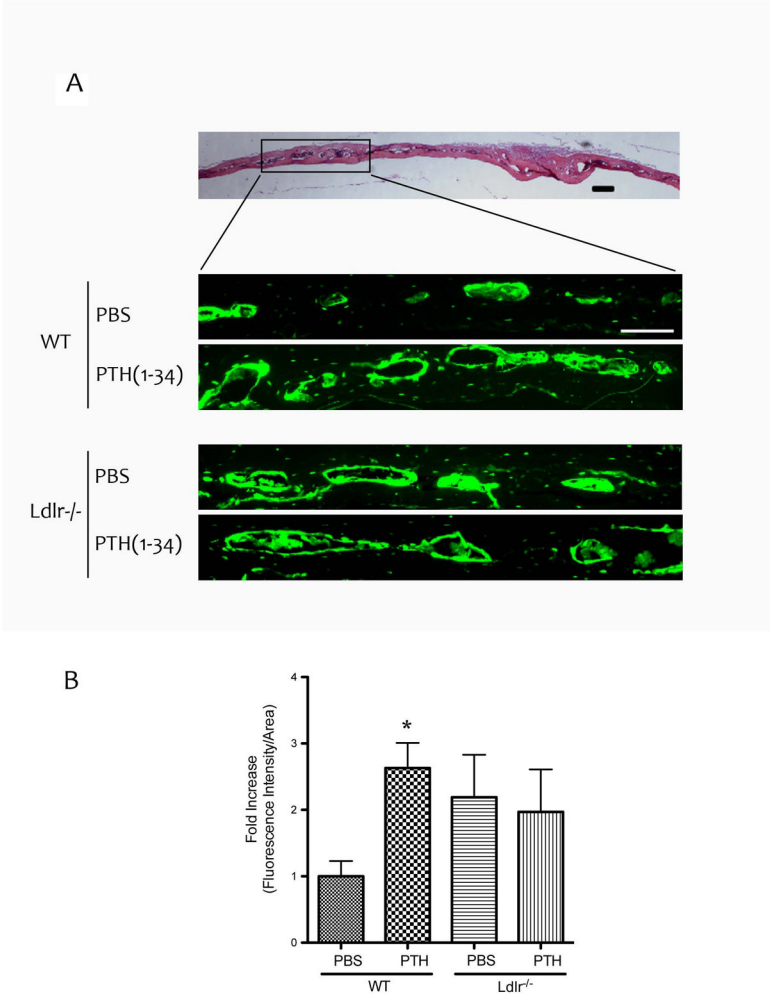

Figure 2. Effects of PTH(1-34) on osteoblasts in calvarial bone

(A) Top panel – hematoxylin and eosin histochemical staining of calvarial bone. Bottom panels – fluorescence images (Topaz filter) of the areas marked by the black rectangular box. (B) Quantitation by Metamorph image analysis. Magnification bar − 200 μm. $^{*}p < 0.05$ vs. respective PBS-treated controls.

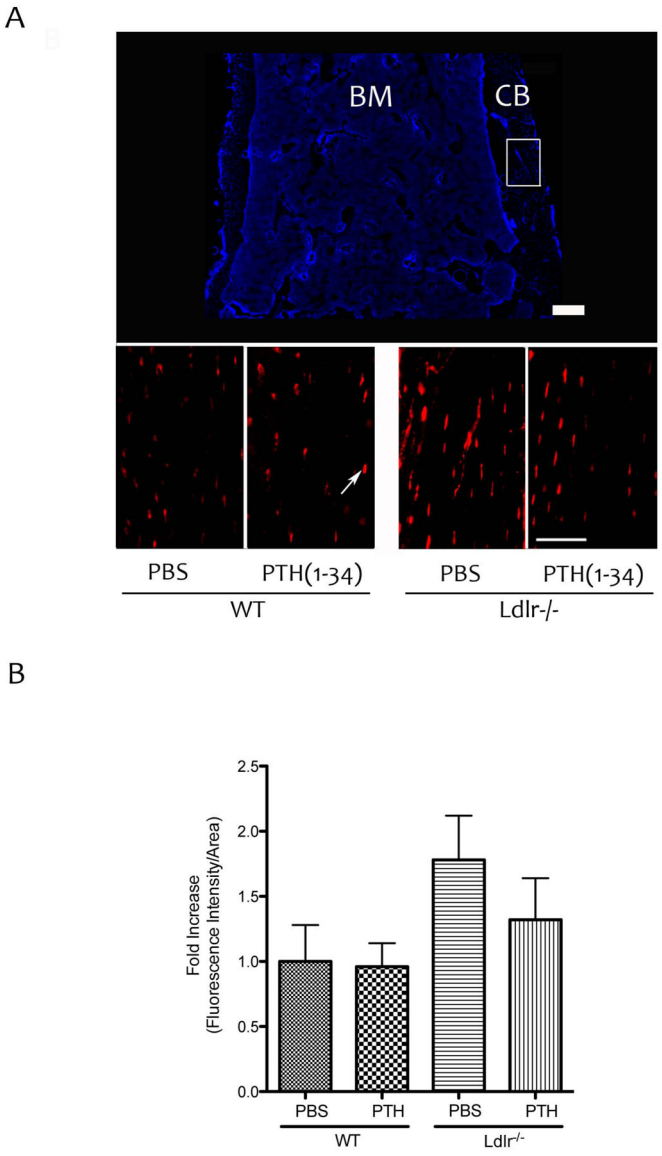

Figure 3. Effects of PTH(1-34) on GFP-labeled osteocytes

(A) Top panel – DAPI image of distal femoral bone from Cyan mice [bone marrow (BM), cortical bone (CB)]. Bottom panels – immuno-fluorescence images of the area marked by the white rectangular box using anti-GFP antibody. Arrow indicates fluorescence labeled osteocytes. Magnification bar − 200 μm. (B) Quantitation by Metamorph image analysis.

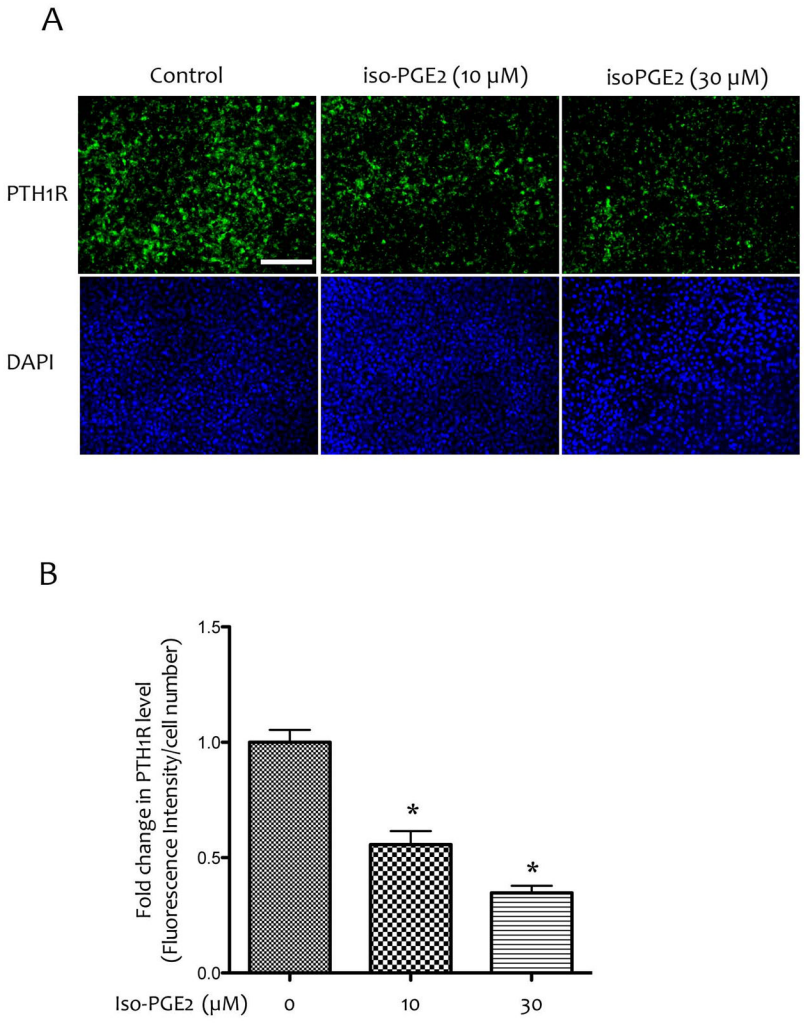

Figure 4. Effects of bioactive inflammatory lipids on PTH1R expression

(A) Immunofluorescence images of MC3T3-E1 cells treated with vehicle or isoPGE2 at 10 μM or 30 μM for anti-PTH1R antibody (top panels) and counterstained with DAPI (bottom panels). Magnification bar − 200 μm. (B) Quantitation by Metamorph image analysis. $^{*}p < 0.05$ vs. vehicle alone.

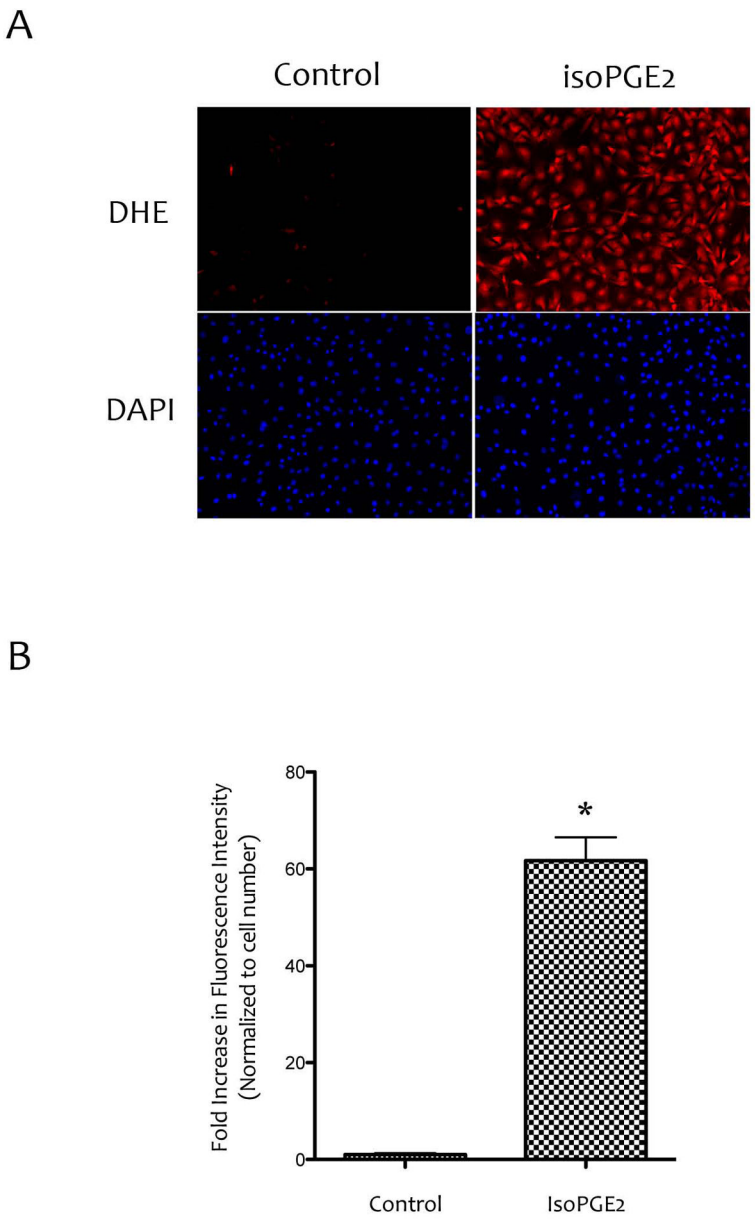

Figure 5. Effects of isoPGE2 on ROS production

(A) Fluorescence images of MC3T3-E1 cells treated with vehicle or isoPGE2 (20 μM) using the ROS indicator dihydroethidium (DHE). Magnification bar − 200 μm. (B) Quantitation by Metamorph image analysis of images shown in (A). $^{*}p < 0.05$ vs. control.

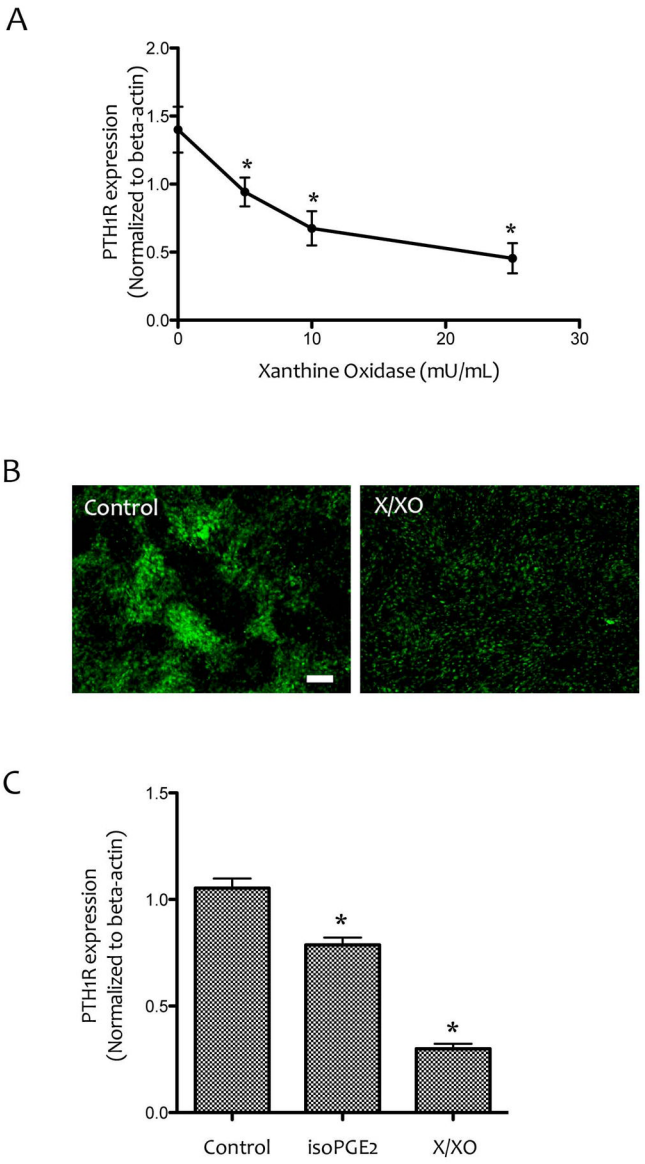

Figure 6. Effects of ROS on PTH1R expression

(A) Realtime RT-qPCR analysis of PTH1R expression in MC3T3-E1 cells treated with xanthine (25 μM) and the indicated concentrations of xanthine oxidase. $^{*}p < 0.05$ vs. control. (B) Immunofluorescence images of MC3T3-E1 cells treated with vehicle or X/XO (25 μM/25 mU/mL) using anti-PTH1R antibody. Magnification bar − 200 μm. (C) Realtime RT-qPCR analysis of PTH1R expression in MC3T3-E1 cells treated with vehicle, isoPGE2 (25 μM) or X/XO (25 μM/25 mU/mL). $^{*}p < 0.05$ vs. vehicle control.

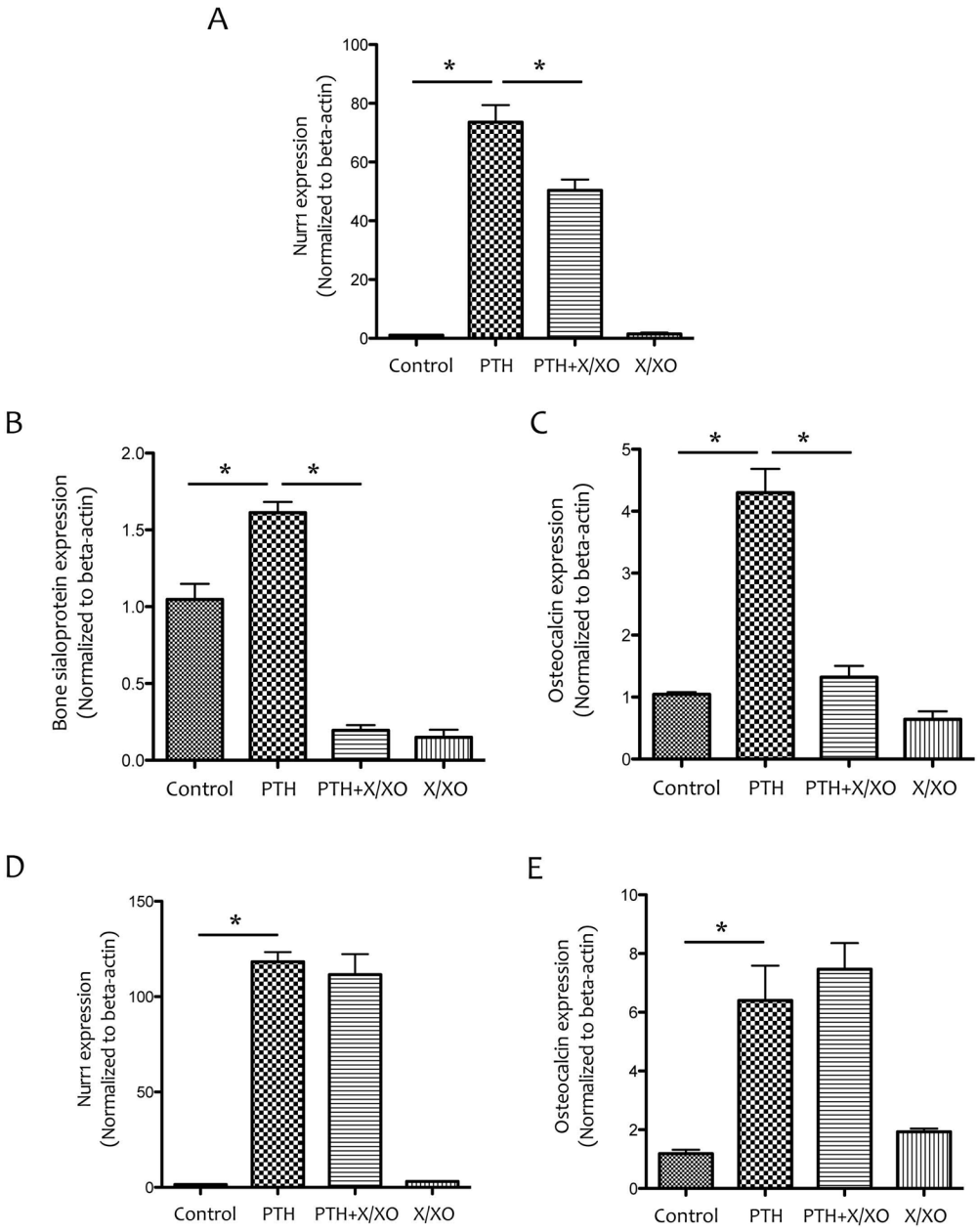

Figure 7. Effects of ROS on PTH-induced gene expression

(A–C) Realtime RT-qPCR analysis of Nurr1, bone sialoprotein and osteocalcin expression in MC3T3-E1 cells pretreated with vehicle or X/XO (25 μM/25 mU/mL) for 6 days followed by co-treatment with vehicle, X/XO and/or PTH (10^{-8}M), as indicated, for an additional 90 min. (D–E) Realtime RT-qPCR analysis of Nurr1 and osteocalcin expression in MC3T3-E1 cells that were cotreated with vehicle, X/XO (25 μM/25 mU/mL) and/or PTH (10^{-8}M) for 90 min after 6 days in culture. $^{*}p < 0.05$.

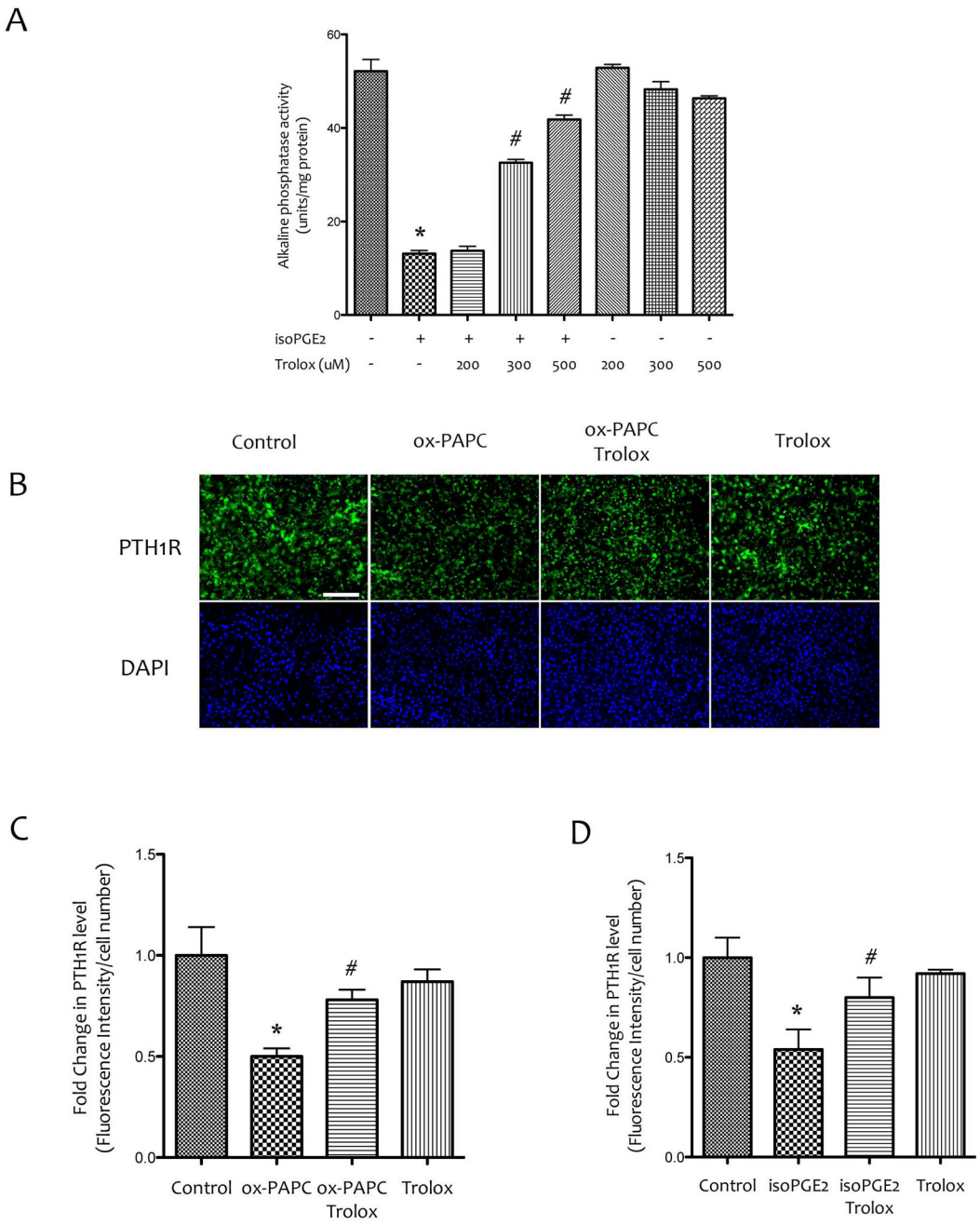

Figure 8. Effects of antioxidants on the inhibitory effects of bioactive inflammatory lipids

(A) Alkaline phosphatase activity of MC3T3-E1 cells that were pretreated with vehicle or Trolox at the indicated concentrations for 1 hr followed by co-treatment with Trolox and isoPGE2 for 6 days. (B) Immunofluorescence images of MC3T3-E1 cells that were pretreated with vehicle or Trolox (400 μM) for 1 hr, followed by co-treatment with vehicle, ox-PAPC (10 μg/ml) and/or Trolox for 6 days. Magnification bar − 200 μm. (C) Quantitative analysis of PTH1R immunofluorescence shown in (B). (D) The levels of PTH1R in MC3T3-E1 cells that were pretreated with vehicle or Trolox (400 μM) for 1 hr, followed by cotreatment with vehicle, isoPGE2 (30 μM) and/or Trolox for 6 days.

Fluorescence images were quantified using Metamorph image analysis. $^{*}p < 0.05$ vs. vehicle, $^{\#}p < 0.05$ vs. isoPGE2 or ox-PAPC.